SURFACE DEGRADATION OF TUNGSTEN FOR PLASMA-FACING COMPONENTS AFTER THERMAL LOADING

[1]Roman PETRÁŠ, [1]Mark MURTAZIN, [2]Matěj PETERKA, [2]Jiří MATĚJÍČEK, [3]Michal HAJÍČEK, [4]Petr HAVLÍK, [3]Ondřej ČÍŽEK, [3]Jiří ZÝKA, [1]Ladislav VÁLA

[1]Research Centre Řež, Husinec-Řež, Czech Republic, EU, roman.petras@cvrez.cz

[2]Institute of Plasma Physics of the Czech Academy of Sciences, Prague, Czech Republic, EU, peterka@ipp.cas.cz

[3]UJP PRAHA a.s., Prague, Czech Republic, EU,hajicek@ujp.cz

[4]Faculty of Mechanical Engineering, Brno University of Technology, Brno, Czech Republic, EU, 107222@vutbr.cz

https://doi.org/10.37904/metal.2024.4966

Abstract

During the operation of fusion devices, plasma facing components (PFCs) are subjected to high thermal loads. These result in mechanical stresses and various forms of degradation and microstructural changes in the material volume. In order to assess the viability of the PFC candidate materials, tungsten samples were subjected to high heat flux tests simulating heat load pulses caused by plasma instabilities. The presented study includes also a thermal model developed in ANSYS Fluent software to simulate the temperature profile at different depths of the sample and its evolution during the tests. Thermal loading was performed using an electron beam facility. Short pulses (~1 s) of up to 40 MW/m^2 thermal load were applied to the top surface of 10 mm wide cylindrical samples. Homogeneous heat flux distribution over the circular area was achieved by scanning the electron beam in a dense pattern. The temperature evolution during the tests was monitored using a thermocouple inserted into the sample along with the surface temperature measurement with a pyrometer. Scanning electron microscopy was used to document surface degradation. A dense net of intergranular cracks typically formed on the loaded surface of the studied material. As a result of a qualitative comparison of the measured temperature profiles during the experiments with the profiles issued from ANSYS simulations, the computational thermal model was verified.

Keywords: Tungsten, plasma facing materials, high heat flux testing, electron beam, surface degradation

1. INTRODUCTION

One of the most significant challenges and key issues for the future fusion facilities, including fusion reactors ITER and DEMO, is the ability of the first wall materials to withstand high thermal loads. During their operation, the plasma facing materials (PFMs) are expected to be subjected to demanding environmental conditions corresponding to steady state (up to 10 MW/m^2), slow transient (up to 20 MW/m^2) or fast transient (up to 1 GW/m^2) thermal loads [1]. In addition to thermal loads, PFMs will face neutron irradiation that can lead to microstructural changes such as the formation of dislocation loops, voids, and precipitation along with the changes in material composition due to transmutations [2, 3].

For this reason, use of materials with specific properties such as high melting point, high sputter resistance, high thermal conductivity and low neutron activation is required. Therefore, tungsten and tungsten-based materials are foreseen to be a prime candidate for this application [4]. Nonetheless, tungsten exhibits major drawback due to its brittleness at low temperature along with the susceptibility to cracking under repeated thermal loads given by its low ductility [2, 5].

When tungsten is exposed to localized high thermal load, generated in experimental conditions, for instance, by an incidental electron, ion or laser beam, the focal spot gets heated to very high temperature within a few seconds. The heated surface expands thermally, resulting in development of high compressive stresses due to surrounding colder material. If the compressive stresses exceed the flow stress (yield strength) of the material, irreversible plastic deformation of the heated region occurs, and the surface is deformed by swelling. Just after the localized and short time exposure, the material shrinks while cooling down to the ambient temperature of the component. As the exposed area of the material is plastically deformed, the material does not return to the initial state resulting in formation of a tensile stresses. If these stresses are higher than the tensile strength of the material, or the accumulated deformation cannot be relaxed, cracking occurs, preferably at weak locations such as grain boundaries when returning to its brittle state at lower temperatures [6, 7]. On the contrary, the development of a fine crack network may prevent further erosion by allowing partial expansion and contraction of the material during the subsequent thermal loading [7].

Other mechanisms of surface degradation have been commonly identified when the material is subjected to thermal loading. The slip bands typically form on the surface of the material, as a consequence of the activation of parallel slip systems during the cyclic plastic deformation when the material is cyclically thermally loaded [6]. Thermal grooving can be recognized on the sample surface as bulging of the neighbouring grains from the grain boundary caused by diffusion processes to equilibrate interfacial forces and to minimize interfacial energies at the groove root [8]. Recrystallization of tungsten can be observed once the temperature of recrystallization is reached during repeated exposures. In this case, a change of the near surface microstructure in the form of grain growth can be recognized [9]. Recrystallized tungsten is coupled with the significant decrease in yield and tensile strength, making it less resistant to thermal shock [1, 9].

The intention of the presented work is to document the surface degradation of tungsten material for plasma facing components after thermal loading generated with an electron beam. To simulate the detrimental events for material caused by high heat flux loads from plasma instabilities, one tungsten sample was subjected to a single pulse of 15 MW/m^2 of thermal load while another tungsten sample underwent three sequential pulses with thermal loads of 10, 20 and 40 MW/m^2. In addition to a single pulse loading, some samples were cyclically loaded to compare the surface degradation after thermal fatigue. The presented study includes also a thermal model developed in ANSYS Fluent software to simulate the temperature profile at different depths of the sample and its evolution in time during the tests.

2. EXPERIMENT

2.1 Material and sample

In this work, tungsten material (99.97% purity) manufactured by Plansee SE was investigated. The material was delivered in form of a rod with diameter of 30 mm and length of 700 mm. The tungsten was produced by powder metallurgy and subsequently normalized by forging. Additional material treatment was not carried out.

A representative microstructure of tungsten is documented in **Figure 1. Figure 1a** shows an electron backscatter diffraction (EBSD) image of tungsten oriented perpendicularly in relation to the rod axis (T-cross-section) illustrating a microstructure consisting of equiaxed grains with average grains size of ~23 μm. The microstructure of tungsten cross section oriented parallelly in relation to the rod axis (L-cross-section) exhibited a texture with elongated grains oriented in the direction of rod axis having average grain size of ~ 80 μm, see **Figure 1b**.

The samples for thermal loading were machined from the tungsten rod to the shape of cylinders parallel to its axis with a height and diameter of 10 mm. The samples were cut by electric discharge machining and the sample surface was mechanically polished. A 5 mm deep hole for the insertion of a thermocouple was produced on the bottom of the sample.

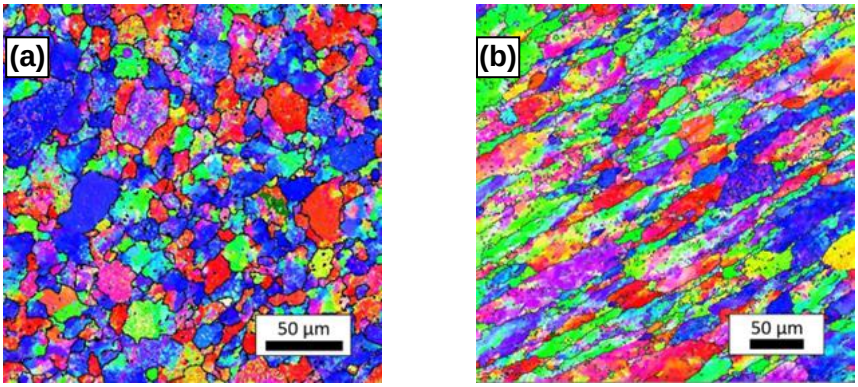

Figure 1 EBSD image of polished (a) T- and (b) L- cross-section produced from tungsten

2.2 Experimental procedure and thermal model

Thermal loading experiments were performed using an electron beam welding (EBW) device, a Pro-Beam EBG 60-150 K26, equipped with a vacuum chamber. Samples with attached thermocouples were placed on a specially designed grid-shaped holder which significantly reduces heat conduction from the samples towards the holder. In addition to measuring the temperature in the material volume using K-type thermocouples, a pyrometer was used to measure the surface temperature. The effective emissivity for the pyrometer was calibrated by matching the temperature measured with the pyrometer and with the thermocouple during the phase of sample cooling via heat radiation when the electron beam was turned off. Measurement spot of the pyrometer covered about 50% of the heated sample surface around its centre and the temperature can only be evaluated in the range of (350, 1800) °C.

During the high heat flux tests the samples were subjected to thermal loads of 10, 15, 20 and 40 MW/m^2. These values were evaluated using the power absorption coefficient of 0.55. The electron beam was scanned across an exposed area of 9.5 mm diameter in a dense pattern of 75 concentric circles to ensure homogeneous heating of the sample surface. The samples were heated by short pulses with duration between 0.35 to 2.2 s depending on the amplitude. Three types of loading are included in the presented work: (1) the sample exposed to a single pulse of 2.2 s at 15 MW/m^2, (2) the sample exposed to three pulses with respective thermal load of 10, 20 and 40 MW/m^2, and finally, (3) the sample cyclically loaded by thermal load of 10 MW/m^2 (10 cycles in total).

In parallel, a thermal model was developed in ANSYS Fluent software to simulate the temperature at different depths of the sample and its evolution during both the heat flux loading of the sample and the cooling phase. Temperature dependent thermal properties of tungsten were used. The heat flux absorbed by the sample surface, determined by the absorption coefficient, was subsequently refined through matching of the modeled temperature evolutions with those obtained in the experiment (**Figure 2**).

3. RESULTS

3.1 Heat flux testing

The temperature profiles during the tests of the tungsten samples subjected to the thermal loads of 15 and 40 MW/m^2 are shown in **Figure 2a** and **2b**, respectively. The temperature record is given from the surface temperature measurements with the pyrometer (red curve) and from the thermocouple inserted approx. in the centre of the sample (black curve). The temperature profiles calculated using the ANSYS thermal model are also shown for the sample surface (green curve) and volume (blue curve).

The surface temperature shows a rapid and immediate growth from the start of the thermal loading pulse and a sharp peak at the end of the pulse. The rise of the volume temperature stays behind the surface due to the significant temperature gradient in the sample during the thermal loading. This gradient, which is much larger in case of 40 MW/m^2, vanishes quickly after the end of pulse, which is observed as a rapid drop in surface temperature. After the whole sample reaches thermal quasi-equilibrium, its temperature decreases in a much longer time scale. The dominant sample cooling mechanism is the radiative heat transfer, owing to the high temperature and minimized thermal contact with the sample holder.

The experimental data correspond generally well to the ANSYS model, which has been adjusted in its boundary conditions to represent the realistic physical conditions as closely as possible. In particular, the effective emissivity of the sample has been adjusted in the model in order to fit sample cool down, and the power absorption coefficient was increased by 10% to fit the overall amplitude of the temperature increase in the volume. A slightly higher value of power absorption coefficient than the originally assumed value of 0.55 for tungsten is within the range reported in [10].

The remaining discrepancies between the thermal model and experimental data can be explained by the uncertainties in temperature measurement with pyrometer and thermocouples. Since the temperature range of the pyrometer is (350,1800) °C, the ANSYS model provides us the missing information on the maximum surface temperature in case of high heat flux loading of 40 MW/m^2.

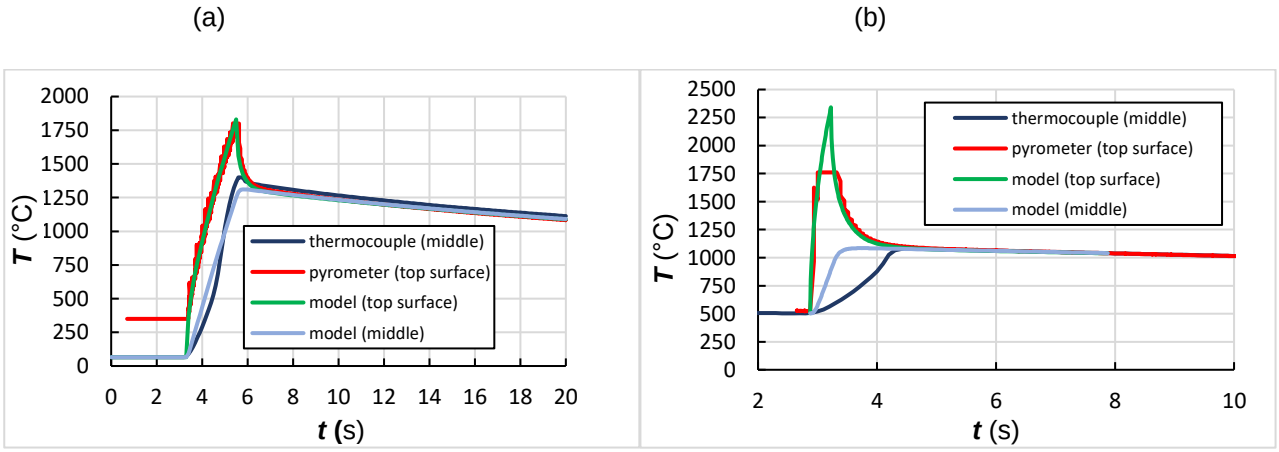

Figure 2 Temperature profile of the samples during the testing with (a) 15 MW/m^2 and (b) 40 MW/m^2 thermal loads. It should be noted that the pyrometer measurement range is about 350 °C to 1800 °C, therefore, temperatures below and above these limits are not recorded.

3.2.1 SEM analysis

Representative SEM images of the samples surface after thermal loading are depicted in **Figures 3, 4** and **5**. **Figure 3** shows the sample surface after a 2.2 s long exposure to thermal load of 15 MW/m^2 (initial temperature was 200 °C, maximum surface temperature was 1800 °C). Typically, the network of intergranular cracks can be observed on the sample surface in the loaded area. Inspection under higher magnification revealed intergranular crack propagation along the grain boundaries of both fine and large grains. A cross-section of the sample shows the depth of intergranular cracks, which is estimated to be approximately 20 μm.

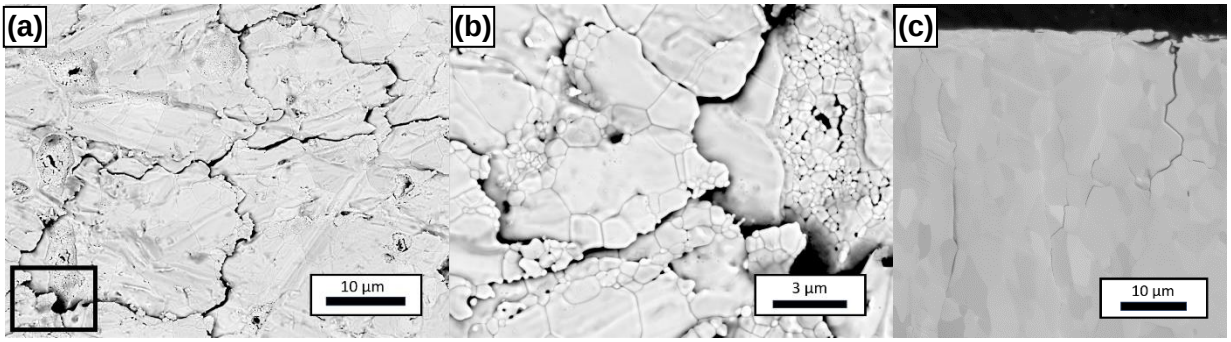

Figure 3 (a) SEM image of the sample surface after exposure to thermal load of 15 MW/m^2. (b) Detail of the area marked in (a). (c) Cross-section showing the cracks propagating vertically in the material volume.

The dense net of intergranular cracks on the sample surface subjected to a sequential thermal load consisting of three pulses with 10, 20 and 40 MW/m^2 (initial temperature was 500 °C; according to the model, the estimated maximum surface temperature was 2340 °C, see **Figure 2b**) is shown in **Figure 4**.

An area free of fine intergranular surface cracks and post-machining groves is observed in the centre of the sample, likely in consequence of the last pulse, which reached the highest surface temperate. **Figure 4b** shows the interface of this area with the rest of the sample. The average grain size in these two areas is similar. We assume that the local temperature exceeded the melting temperature for a very short time, resulting in so-called healing of the sample surface by small-scale melting and solidification. Although the maximum surface temperature does not exceed 2500 °C according to the ANSYS model, this value has to be considered as space-averaged, and some local overheating can be expected due to the limited temporal homogeneity of the applied heat flux. In fact, for this case of the highest applied average heat flux, a transient surface temperature increase of about 1000 °C during an interval as short as 10 µs is predicted by an analytical model of 1D heat conduction of the thermal energy deposited in the central area during a single cycle of electron beam scanning, with a heat penetration depth of about 15 µm.

Large cracks observed in the central area of the sample are believed to be formed during the cooling of the sample after exposure to relieve the thermally induced stresses. In addition to small cracks, which typically propagate intergranularly from the surface and reach a depth of up to 50 µm, a long well-evolved crack (400 µm) can be recognized on the cross-section in **Figure 4c**.

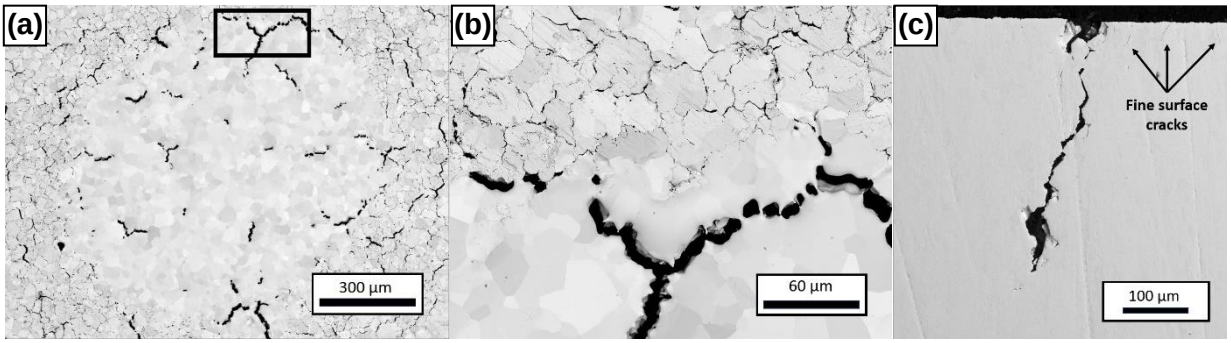

Figure 4 (a) SEM image of the sample surface after exposure to thermal load of 40 MW/m^2. (b) Detail of the area marked in (a). (c) Cross-section showing the fine cracks along with well-developed crack propagating in the material volume.

The sample surface after 10 thermal loads of 10 MW/m^2 (initial temperature was 500 °C, maximum surface temperature was 1200 °C) is documented in **Figure 5**. The net of the intergranular cracks developed on the surface appears to be similar to the surface of the sample subjected to the single thermal load of 15 MW/m^2. Across-section of the sample shows an intergranular crack propagating to the depth of ~40 μm. Closer inspection of the loaded surface revealed significant bulging of the material along the grain boundaries related to thermal grooving, see **Figure 5b**. The formation of bulging is characteristic of plastically cyclically loaded surfaces [6, 7].

Cyclic thermal loading can lead to thermal fatigue degradation of the material surface in the form of surface roughening. The morphology of some grains differs as the slip bands can be observed on some grains. The slip bands are developed in parallel within a single grain and are related to the crystallographic orientation of individual grains. The formation of the slip bands is driven by activation of slips systems during the cyclic plastic deformation, and with further thermal loading, slip bands are more pronounced and frequent in other grains [11].

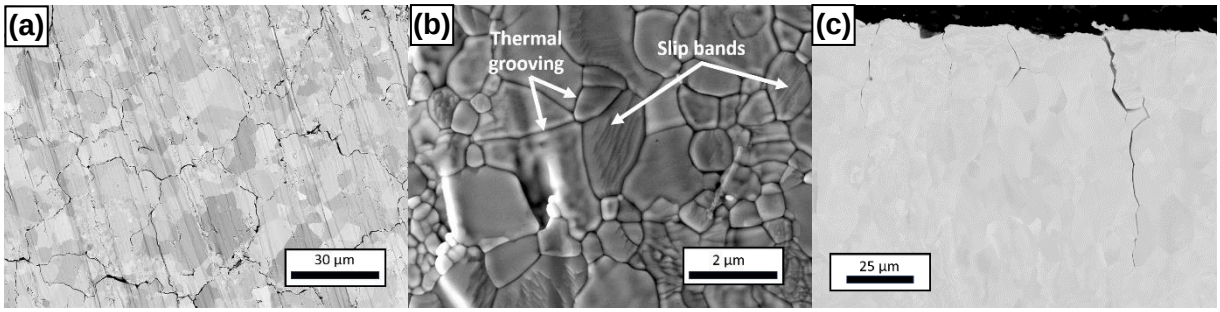

Figure 5 (a) SEM image of the sample surface after 10 thermal loads of 10 MW/m^2. (b) Detail showing thermal grooving and slip bands. (c) Cross-section showing the cracks propagating in the material volume.

Since the thermal fatigue resistance of tungsten is a critical parameter for the assessment of the component lifetime, there is an effort to understand the mechanisms of surface degradation leading to premature crack initiation. The combination of various thermal loads and cycle index has been investigated [11, 12]. An increase in the number of cycles along with the thermal load results in formation of slip bands consisting of extrusions and intrusions [6, 11]. An intrusion represents a crack-like defect from which the crack initiates [13]. In this case two potential mechanisms of early crack formation can operate: cracking of the grain boundaries and transgranular crack formation from a deepening intrusion. However, the direct clear evidence of transgranular cracking is missing. Bearing in mind the ductile to brittle transition temperature (DBTT), the base temperature represents an important parameter to consider. Yuan et al. [12] studied the effect of the base temperature on surface roughening. The surface roughening became more significant when the base temperature was increased from room temperature to 400 °C. This corresponds to a higher level of plasticity due to thermal activation of dislocation motion when compared to room temperature. In the case of our measurements, the base temperate was well above the DBTT of tungsten, so the influence of the base temperature on surface roughness cannot be inferred.

4. CONCLUSION

Surface degradation of tungsten after high heat flux testing with different thermal loads has been studied by means of an electron beam facility. In general, a dense net of intergranular cracks can be observed on the sample surface within the loaded area regardless of the loading conditions. Inspection of a cross-section revealed well-developed cracks (up to 400 μm) propagating in an intergranular manner only when exposed to the highest thermal load. Tungsten subjected to cyclic thermal loading exhibited surface roughening in a form

of thermal grooving and slip bands. A thermal model in ANSYS Fluent was developed to simulate the temperature at different depths of the sample and time evolution of temperature during and after thermal loading. The observed temperature evolution during the measurements corresponds to the developed thermal model within the known sources of uncertainty.

ACKNOWLEDGEMENTS

This work was supported by Technology Agency of the Czech Republic through grant no. TK03030045.

The presented results were obtained using the CICRR infrastructure, which is financially supported by the Ministry of Education, Youth and Sports - project LM2023041.

REFERENCES

[1] WIRTZ, M., CEMPURA, G., LINKE, J., PINTSUK, G., UYTDENHOUWEN, I. Thermal shock response of deformed and recrystallised tungsten. *Fusion Engineering and Design*. 2013, vol. 88, pp 1768-1772.

[2] TERRA, A., SERGIENKO, G. et al. Micro-structuring of tungsten for mitigation of ELM-like fatigue. *Physica Scripta.* 2020,T171, 014045.

[3] GILBERT, M.R., ARAKAWA, K. et al. Perspectives on multiscale modelling and experiments to accelerate materials development for fusion. *Journal of Nuclear Materials.* 2021, vol. 554, 153113.

[4] BREZINSEK, S., COENEN, J. et al. Plasma–wall interaction studies within the EURO fusion consortium: progress on plasmafacing components development and qualification. *Nuclear Fusion.* 2017, vol. 57, 116041.

[5] MEROLA, M., LOESSER, D. et al. ITER plasma-facing components. *Fusion Engineering and Design.* 2010, vol. 85, pp. 2312-2322.

[6] SILLER, M., SCHATTE, J., GERZOSKOVITZ, S., KNABL, W., PIPPAN, R., CLEMENS, H., MAIER-KIENER, V. Microstructural evolution of W-10Re alloys due to thermal cycling at high temperatures and its impact on surface degradation. *International Journal of Refractory Metals and Hard Materials.* 2020, vol. 92, 105285.

[7] LINKE, J., LOEWENHOFF, T., MASSAUT, V., PINTSUK, G., RITZ, G., RÖDIG, M., SCHMIDT, A., THOMSER, C., UYTDENHOUWEN, I., VASECHKO, V., WIRTZ, M. Performance of different tungsten grades under transient thermal loads. *Nuclear Fusion.* 2021, vol. 51, 073017.

[8] HAREMSKI, P., EPPLE, L., WIELER, M., LUPETIN, P., THELEN, R., HOFFMANN, M.J. A thermal grooving study of relative grain boundary energies of nickel in polycrystalline Ni and in a Ni/YSZ anode measured by atomic force microscopy. *Acta Materialia.* 2021, vol. 214, 116936.

[9] LOEWENHOFF, Th., BARDIN, S., GREUNER, H., LINKE, J., MAIER, H., MORGAN, T.W., PINTSUK, G., PITTS, R.A., RICCARDI, B., DE TEMMERMANG. Impact of combined transient plasma/heat loads on tungsten performance below and above recrystallization temperature. *Nuclear Fusion.* 2015, vol. 55, 123004.

[10] WIRTZ, O.M. *Thermal shock behaviour of different tungsten grades under varying conditions.* Aachen, 2012. Dissertation. RWTH Aachen University.

[11] WANG, L., WANG, B., LI, S.-D., MA, D., TANG, Y.-H., YAN, H. Thermal fatigue mechanism of recrystallized tungsten under cyclic heat loads via electron beam facility. *International Journal of Refractory Metals and Hard Materials.* 2016, vol. 61, pp 61-66.

[12] Y. YUAN, Y., DU, J., WIRTZ, M., LUO, G.-N., LU, G.-H., LIU, W. Surface damage and structure evolution of recrystallized tungsten exposed to ELM-like transient loads. *Nuclear Fusion.* 2016, vol. 56, 036021.

[13] POLÁK, J., PETRÁŠ, R., CHAI, G., ŠKORÍK, V. Surface profile evolution and fatigue crack initiation in Sanicro 25 steel at room temperature. *Materials Science and Engineering.* 2016, vol. 658, pp 221-228.